Materials Letters 236 (2019) 252–255

Contents lists available at ScienceDirect

Materials Letters

journal homepage: www.elsevier.com/locate/mlblue

Effect of thermal annealing and irradiation damage on the superconducting critical temperature of nanocrystalline γ-Mo_2N thin films

N. Haberkorn [a,b,*], S. Bengio [a], S. Suárez [a,b], P.D. Pérez [a], J.A. Hofer [b], M. Sirena [a,b]

[a] Comisión Nacional de Energía Atómica and Consejo Nacional de Investigaciones Científicas y Técnicas, Centro Atómico Bariloche, Av. Bustillo 9500, 8400 San Carlos de Bariloche, Argentina

[b] Instituto Balseiro, Universidad Nacional de Cuyo and Comisión Nacional de Energía Atómica, Av. Bustillo 9500, 8400 San Carlos de Bariloche, Argentina

ARTICLE INFO

Article history:
Received 14 September 2018
Accepted 15 October 2018
Available online 15 October 2018

Keywords:
Nitrides
Sputtering
Superconductivity
Irradiation

ABSTRACT

We report on the influence of the disorder and stoichiometry in the resulting superconducting critical temperature of γ-Mo_2N thin films. Initially, three films (with T_c values of 7.6 K, 6.8 K and 6 K) were grown at room temperature by reactive sputtering, on Si (1 0 0) using different N_2/(Ar+N_2) mixtures. The influence of the thermal annealing up to 973 K and irradiation damage produced by 1 MeV Zr^+(fluence up 2×10^{14} cm^{-2}) is analyzed. The T_c of pristine films remains unchanged for increasing irradiation doses up 2×10^{14} cm^{-2}. The T_c for annealed films decreases close to the value expected for bulk samples (≈5 K) for increasing the annealing temperature. Successive irradiations of the annealed films tend to increase their T_c up to its initial values (before annealing). The results indicate that the T_c in nanometric grain size γ-Mo_2N thin films is affected by both nitrogen stoichiometry and disorder at the atomic scale.

1. Introduction

Molybdenum nitrides have attracted much attention as superconducting materials due to their potential application in tunnel junctions and radiation detectors [1–3].The Mo nitrides present several superconducting crystalline phases: γ-Mo_2N (cubic) with superconducting critical temperature $T_c \sim 5$ K [4], β-Mo_2N (tetragonal) with $T_c \sim 5$ K [5] and δ-MoN (hexagonal) with $T_c \sim 12$ K [6,7]. A distinctive property of γ-Mo_2N thin films is that its T_c is increased from ≈ 5 K to 8 K by disorder [8,9]. This effect may be related to variations in the electronic density of states at the Fermi level $N(0)$ [10]. In addition to the disorder, the T_c in nanocrystalline γ-Mo_2N_{1+x}($0 \leq x \leq 0.4$) thin films grown by reactive sputtering at room temperature drops from 8 K to ≈5.8 K due to changes in the nominal nitrogen stoichiometry [11,12]. Considering that changes in the nitrogen content may affect the disorder at the nanoscale (with the coexistence of crystalline and amorphous regions), the influence of each mechanism on the T_c is unclear.

In this work, we analyze the influence of nitrogen stoichiometry and disorder on the T_c of Mo_2N_{1+x} thin films grown by reactive sputtering on Si (1 0 0). The T_c values of films grown with three different Ar:N_2 mixtures are compared with those obtained after thermal annealing at 873 K and 973 K and successive irradiations with 1 MeV Zr ions. The zirconium was selected considering that due to its higher charge may produce more displacement per atom that other light ions such as protons (for the same doses). The results show that the T_c of pristine films (highly disordered) systematically decreases to values down below 5 K with thermal annealing. The irradiations have a negligible influence on the T_c of pristine films, but for the annealed ones, its value systematically increases to the ones observed before the irradiation, for increasing irradiation doses.

2. Material and methods

Mo_2N_{1+x}films were deposited by DC reactive magnetron sputtering on Si (1 0 0) [11,12]. No intentional heating of the substrate was used. Films were grown from a pure Mo target in a N_2/(Ar+N_2) gas mixture with N_2 partial pressure going from 8%, 15% and 25% of the mixture's 5 mTorr pressure. The expected nominal chemical composition of the films is Mo_2N_{1+x} with x = 0.05, 0.15 and 0.33 (increasing N_2 in the gas mixture [12]). Wherever used, the notation [MoNY] indicates a Mo-N film grown with Y% N_2 partial pressure. The notation [MoNY]*AT*, [MoNY]*IF* and [MoNY]*ATIF* indicates if the films are annealed at *T* K, irradiated with fluences *F* = 1 or 2

* Corresponding author at: Comisión Nacional de Energía Atómica and Consejo Nacional de Investigaciones Científicas y Técnicas, Centro Atómico Bariloche, Av. Bustillo 9500, 8400 San Carlos de Bariloche, Argentina.

E-mail address: nhaberk@cab.cnea.gov.ar (N. Haberkorn).

https://doi.org/10.1016/j.matlet.2018.10.094
0167-577X/

(see description below), and annealed and irradiated, respectively. The film thicknesses (determined from low angle X-ray diffraction) were 70 nm, 67 nm, and 66 nm for [MoN8], [MoN15] and [MoN25], respectively.

X-ray (XRD) diffraction data were obtained using a Panalytical Empyrean equipment. Irradiation with 1 MeV Zr^+ produces mostly Frenkel pairs, i.e. random point defects. The irradiation was performed in two sequential steps of 1×10^{14} cm^{-2} (IRR1 = 1×10^{14} cm^{-2} and IRR2 = 2×10^{14} cm^{-2}). The irradiations were performed with the ion beam perpendicular to the surface of the films. The energy of the ions was selected to place the Bragg peak inside the substrate (as estimated using the SRIM code [13]). Surface composition analysis was performed by means of X-ray photoelectron spectroscopy (XPS). The electrical transport measurements were performed using the standard four-point configuration.

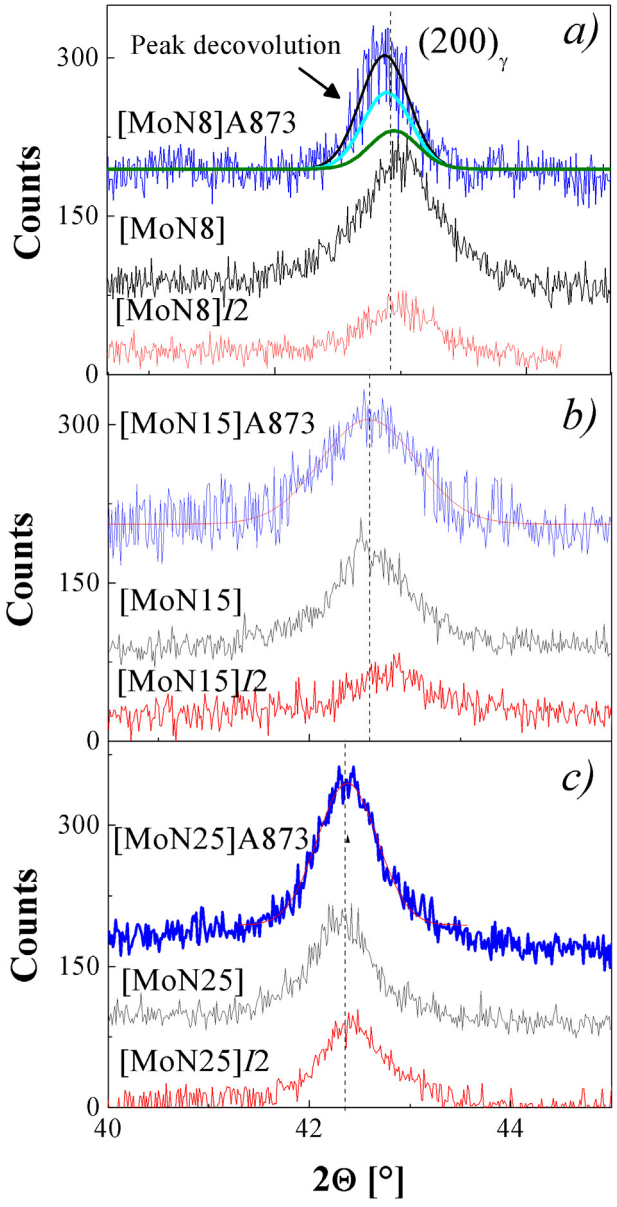

Fig. 1. XRD pattern for pristine, irradiated with 1 MeV Zr (fluence 2×10^{14} cm^{-2}) and annealed γ-Mo_2N thin films. Ar: N_2 mixture with: *a)* 8% N_2; *b)* 15% N_2; *c)* 25% N_2.

3. Results and discussion

Fig. 1a–c shows the XRD patterns for [MoNY], [MoNY]*I*2 and [MoNY]*A*973, respectively. The 200 reflection corresponding to the cubic γ-Mo_2N phase is observed. The peak is systematically shifted to smaller angles when the N_2 partial pressure is increased, which is related with a larger *a* lattice parameter [12]. The films are mainly textured along the (1 0 0) axis. Small (1 1 1) reflections are present in [MoN15] and [MoN25] (see Supplementary Material). The average crystallite size estimated from Scherrer's equation (considering separately $CuK_{\alpha 1}$ and $CuK_{\alpha 2}$) with the [2 0 0] reflection is shown in Table 1. Thermal annealing has a weak influence in the grain size average, which ranges between 20 nm and 30 nm. These values are consistent with previously published high-resolution transmission electron images [11].

The oxidation state of Mo in pristine, annealed and irradiated films was analyzed by XPS measurements. The Mo3d spectrum provides information about the oxidation states and chemical composition [14–17]. Fig. 2a–c show the Mo3d spectra for [MoN25]*A*973, [MoN25]*I*2 and [MoN25], respectively. The curves for [MoN25] and [MoN25]*I*2 correspond to the surface cleaned with Ar^+ sputtering (2 kV), which reduce the superficial MoO_3 components [11]. Similar spectrums were obtained for [MoN8] and [MoN15]. The elemental spectra are composed by two identical peaks that correspond to the spin-orbit split $3d_{5/2}$ and $3d_{3/2}$ for Mo, with relative intensities of 3:2. The spectra were fitted using a Voight function for each peak plus a Shirley-type background. The spectra display three components: a major component at a binding energy of 228.6 eV (related to $Mo^{\delta+}$ ($2 \leq \delta < 4$) [17]) and minor components at higher binding energies (related to MoO_2 and MoO_3, respectively [15,18]). The component associated to MoO_2 is composed of a screened and an unscreened doublet [19,20]. The irradiation produces an increment in the MoO_3 peak, which can be related to surface modification (activation). The thermal annealing reduces the oxide components at the surface and only remains the $Mo^{\delta+}$ doublet. The small shift at the $Mo^{\delta+}$ component (≈0.2–0.3 eV) observed for the pristine and irradiated films can be related to final state effects due to the presence of oxides that prevents the fast neutralization of the hole created during the photoemission process. No features related to the δ-MoN component are observed in the annealed film [21].

Fig. 3 shows the normalized resistance versus temperature for the studied films. Table 1 shows a summary of the results. The T_c values in pristine films are 7.6 K, 6.8 K and 6 K for [MoN8], [MoN15] and [MoN25], respectively. The residual resistivity ratio

Table 1
Summary of the superconducting critical temperature (T_c), residual resistivity ratio (R^{290K}/R^{10K}) and grain size *D* for the studied films (estimated from the (2 0 0) reflection using the Scherrer equation).

Sample	T_c[K]	*RRR*	*D* [nm]
[MoN8]	7.6	0.98	19 (2)
[MoN8]*I*2	7.6	0.98	20 (2)
[MoN8]*A*873	4.7	1.1	–
[MoN8]*A*973	4.7	–	32 (2)
[MoN8]*A*973*I*2	6.5	1.01	–
[MoN15]	6.8	0.92	22 (2)
[MoN15]*I*2	6.8	0.88	–
[MoN15]*A*873	5.3	0.98	20 (2)
[MoN15]*A*873*I*2	6.7	0.85	–
[MoN15]*A*973	4.1	0.98	–
[MoN15]*A*973*I*2	6.1	0.9	
[MoN25]	6.0	0.88	26 (2)
[MoN25]*I*2	6.0	–	26 (2)
[MoN25]*A*873	5.2	0.95	
[MoN25]*A*973	4.9	0.95	26 (2)
[MoN25]*A*973*I*2	6.0	–	

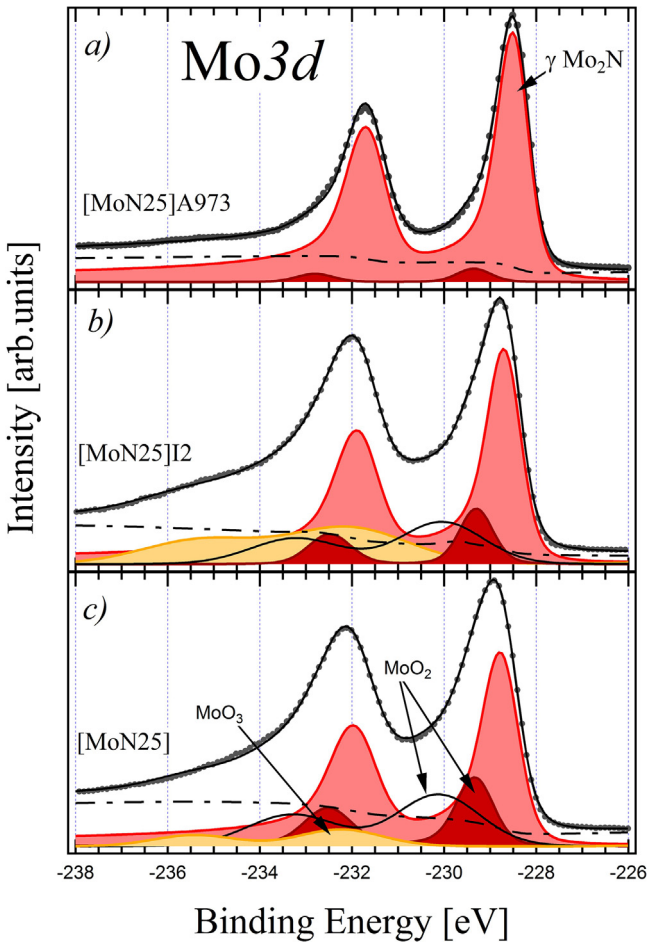

Fig. 2. Mo3d spectra of [MoN25]: *a)* annealed at 973 K; *b)* irradiated with 1 MeV Zr (fluence 2×10^{14} cm^{-2}); and c*)* pristine at 973 K.

($RRR = R^{290K}/R^{10K}$) in pristine films is smaller than 1 (see table 1), which is signature of high disorder with a very short mean free path *l*. After annealing, [MoN8] displays metallic behavior (RRR > 1), whereas *RRR* remains below 1 in [MoN15] and [MoN25]. This indicates that the excess of N respect to Mo_2N (related to interstitial doping with N) contributes to the disorder at the atomic scale, which is also evidenced in the evolution with thermal annealing of the T_c. For [MoN8], the T_c value varies from 7.6 K to 4.8 K after annealing at 873 K and 973 K. However for [MoN15] and [MoN25], the T_c value shows a gradual reduction to values below 5 K after annealing at 873 K and 973 K. The irradiations with Zr^+ ions do not increase T_c for pristine films, but systematically increase the T_c of annealed samples to the ones present before the thermal annealing. The negligible influence of the irradiation on T_c of pristine samples indicates that they are in extremely disordered limit and its T_c value is mainly given by changes in the nitrogen stoichiometry [11]. The gradual reduction in T_c to bulk values produced by thermal annealing have been related to variations in the electronic density of states at the Fermi level *N* (0) [10]. Studies focused in the correlation between the disorder and the band structures are necessaries to understand the changes on the superconducting properties of γ-Mo_2N thin films.

Finally it is important to note that, in the same way than other nanocrystalline metal nitrides [22,23], the high tolerance to the irradiation (evidenced in the electrical transport of pristine films) enhances its potential applications in electronic devices for high-radiation environments.

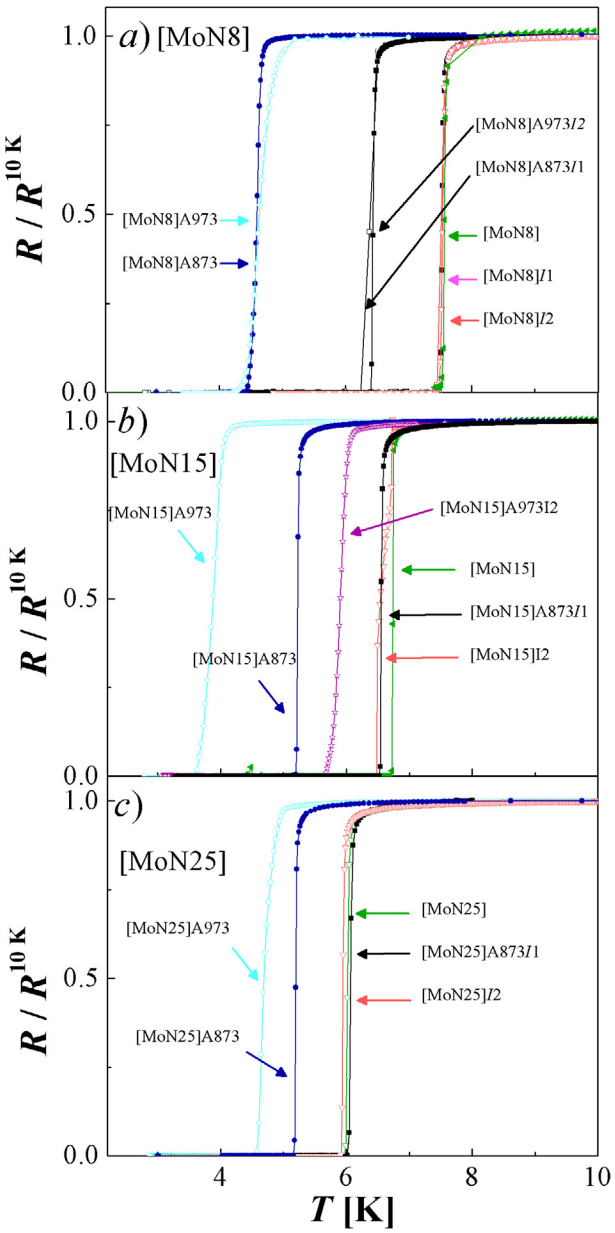

Fig. 3. Electrical transport for *a)* [MoN8]; *b)* [MoN15]; and c*)* [MoN25].

4. Conclusions

In summary, the effects of thermal annealing and irradiation damage in the superconducting critical temperature T_c of nanometric grain size γ-Mo_2N thin films are analyzed. Thermal annealing reduces the disorder at the atomic scale shifting the T_c values to those typically observed in bulk samples. The irradiation of annealed samples tends to recover the T_c displayed by pristine samples, indicating that they are close to an extremely disordered limit and the differences in their T_c are given by differences in the nitrogen stoichiometry.

Acknowledgment

We thank C. Olivares for technical assistance. This work was partially supported by the ANPCYT (PICT 2015-2171), U. N. de Cuyo 06/C505 and CONICET PIP 2015-0100575CO. NH, SB, JAH and MS

are members of the Instituto de Nanociencia y Nanotecnología, CNEA-CONICET.

Appendix A. Supplementary data

Supplementary data to this article can be found online at https://doi.org/10.1016/j.matlet.2018.10.094.

References

[1] A. Shurakov, Y. Lobanov, G. Goltsman, Supercond. Sci. Tech. 29 (2015) 023001.
[2] Sergey K. Tolpygo et al., IEEE Trans. Appl. Supercond. 28 (2018) 1100212.
[3] Chandra M. Natarajan et al., Supercond. Sci. Technol. 25 (2012) 063001.
[4] B.T. Matthias, J.K. Hulm, Phys. Rev. 87 (1952) 799–806.
[5] Kei Inumaru et al., Chem. Mater. 17 (2005) 5935–5940.
[6] Shanmin Wang et al., Sci. Rep. 5 (2015) 13733.
[7] Hanlu Zhang et al., J. Alloys Compounds 704 (2017) 453–458.
[8] Hongmei Luo et al., J. Phys. Chem. C 115 (2011) 17880–17883.
[9] R. Baskaran et al., J. Phys. D 49 (2016) 205304–205307.
[10] W.L. Johnson et al., Phys. Rev. B 18 (1978) 206–2017.
[11] N. Haberkorn et al., Mater. Chem. Phys. 204 (2018) 48–57.
[12] N. Haberkorn et al., Mater. Lett. 215 (2018) 15–18.
[13] J.F. Ziegler, J.P. Biersack, U. Littmark, The Stopping and Range of Ions in Solids, Pergamon, New York, 1985.
[14] Geug-Tae Kim et al., Appl. Surf. Sci. 152 (1999) 35–43.
[15] Z.B. Zhaobin Wei, P. Grange, B. Delmon, Appl. Surf. Sci. 135 (1998) 107–114.
[16] Kejun Zhang et al., Appl. Mater. Interfaces 5 (2013) 3677–3682.
[17] Y.M. Wang, R.Y. Lin, Mater. Sci. Eng. B 112 (2004) 42–46.
[18] Muneyoshi Yamada et al., J. Phys. Chem. 95 (1991) 7037–7042.
[19] Jonas Baltrusaitis et al., Appl. Surf. Sci. 326 (2015) 151–161.
[20] David O. Scanlon et al., J. Phys. Chem C 114 (2010) 4636–4645.
[21] N. Haberkorn et al., Thin Solid Films 660 (2018) 242–246.
[22] L. Jiao et al., J. Appl. Phys. 117 (2015) 145901–145909.
[23] Yong-Qin Chang et al., Front. Mater. Sci. 7 (2013) 143–155.